CHAPTER VII
PARTIAL OXIDATION OF METHANE OVER Ni/Nb-DOPED $Ce_{0.75}Zr_{0.25}O_2$ CATALYSTS

7.1 Abstract

In this study, $Ce_{0.75}Zr_{0.25}O_2$ mixed oxide catalysts and catalyst doped with 1, 5 and 10 wt% Nb were prepared via urea hydrolysis and tested for methane partial oxidation. The XRD patterns of $Ce_{0.75}Zr_{0.25}O_2$ mixed oxide catalysts and Nb-doped indicate a cubic fluorite structure. The evidence for extra peaks due to non-incorporated Nb was not observed in any XRD patterns of Nb-doped $Ce_{0.75}Zr_{0.25}O_2$. The incorporation of 1 wt% Nb was found to promote the reduction of the $Ce_{0.75}Zr_{0.25}O_2$ mixed oxide whereas increasing the amount of Nb (5 and 10 wt%) retarded surface reduction. The methane oxidation activity of the mixed oxides was apparently dependent on Nb loading, which relates to the degree of reducibility. In general the catalytic activity decreased with increasing Nb content.

7.2 Introduction

Cerium oxide or ceria has been widely used as catalyst in many oxidation reactions because of its redox properties and high oxygen storage capacity. Ceria can act as oxygen buffer by shifting between CeO_2 under oxidizing condition and Ce_2O_3 under reducing conditions. However, ceria has a poor thermal stability at high temperatures.

Recently, CeO_2-ZrO_2 mixed oxide has been found to improve the thermal stability of pure ceria and the incorporation of Zr^{4+} into the CeO_2 lattice can modify the redox properties, which can increase the catalytic activity, particularly for oxidation reactions involving lattice oxygen. Otsuka *et al.* (1999) found that the oxygen desorption and reduction by H_2 of $Ce_{1-x}Zr_xO_2$ solid solution with $x \leq 0.5$ took place at lower temperature as compared with pure ceria. In our early study, we have found that $Ce_{0.75}Zr_{0.25}O_2$ solid solution exhibited the highest activity for methane oxidations (Pengpanich *et al.*, 2002).

It is believed that oxygen vacancies and mobile electronic carriers are involved in hydrocarbon oxidation. Stagg-Williams *et al.* (2000) reported that a higher degree of reduction of Ce-doped ZrO_2 catalyst results in an increase in the number of oxygen vacancies and subsequently resists in carbon deposition. Therefore, the impact of oxygen vacancies on catalytic performance of Ce-doped ZrO_2 needs to be better understood.

It was reported that small amounts of niobium oxide species added to mixed oxides can play a role of a promoter as reported in the cases of oxidative dehydrogenation and oxidation of propane (Barbieri *et al.*, 2000; Noronha *et al.*, 2000). Nb cation increases the concentration of mobile electronic carriers and/or fills oxygen vacancies, which can also be expected to influence methane oxidation. In a previous study (Pengpanich *et al*, 2004), we reported that 5 wt%Ni/$Ce_{0.75}Zr_{0.25}O_2$ catalysts showed high activity, selectivity and stability for methane partial oxidation. Furthermore, this catalyst was found to resist to coke formation due to its high degree of metal dispersion and surface oxygen mobility. However, some carbon deposition was still observed.

In this study, we investigated the effect of Nb loading on 5 wt% Ni/$Ce_{0.75}Zr_{0.25}O_2$ catalyst to methane and iso-octane partial oxidation. The solid solution of $Ce_{0.75}Zr_{0.25}O_2$ catalyst along with 1, 5 and 10 wt% Nb-doped via urea hydrolysis were prepared. The catalytic activities of these materials and the influence of Nb on methane and iso-octane partial oxidation are reported.

7.3 Experimental

7.3.1 Catalyst Preparation

Mixed oxide solid solution of $Ce_{0.75}Zr_{0.25}O_2$ was prepared via urea hydrolysis of 0.1 M $Ce(NO_3)_3$ and $ZrOCl_2$ solution at 100°C for 50 h. More details were reported elsewhere (Pengpanich *et al.*, 2002).

Nb-doped $Ce_{0.75}Zr_{0.25}O_2$ mixed oxide supports were also prepared by urea hydrolysis of 0.1 M $Ce(NO_3)_3$, $ZrOCl_2$ and $NbCl_5$. The amount of $NbCl_5$ solution was altered depending on the desired loading of 1, 5 or 10 wt%. The products were then calcined at 500 and 900°C for 4 hr.

The Ni was loaded into the catalyst supports by the incipient wetness impregnation method using the aqueous solutions of $Ni(NO_3)_2 \cdot 6H_2O$. The loading amount of Ni was 5 wt %. The catalysts were then calcined at 500°C for 4 hr in air.

7.3.2 Charaterizations

BET surface area was determined by N_2 adsorption at 77 K (five point Brunauer-Emmett-Teller (BET) method using a Quantachrome Corporation Autosorb-1). Prior to the analysis, the samples were outgassed to eliminate volatile adsorbents on the surface at 250°C for 4 hr.

H_2 uptake and degree of dispersion were determined by using pulse technique (ThermoFinnigan modeled TPDRO 1100). About 250 mg of sample was placed in a quartz reactor. Prior to pulse chemisorption, the sample was reduced in H_2 atmosphere at 500°C for 1 hr. Then the sample was purged with N_2 at 500°C for 30 min and cooled to 50°C in flowing N_2. A H_2 pulse (pure H_2, 0.4 ml) was injected into the sample at 50°C. The metal dispersion was calculated by assuming the adsorption stoichiometry of one hydrogen atom per nickel surface atom.

A Rigagu X-ray diffractometer system equipped with a RINT 2000 wide-angle goniometer using CuK_α radiation and a power of 40 kV x 30 mA was used for examination of the crystalline structure. The intensity data were collected at 25 °C over a 2θ range of 20-90° with a scan speed of 5° (2θ)/min and a scan step of 0.02° (2θ).

H_2-Temperature programmed reduction (TPR) measurements were carried out to investigate the redox properties over the resultant materials. In this study, H_2 was used as a reducing gas. H_2-TPR was carried out in TPR analyzer (Quantachrome model ChemBET- 3000 TPR/TPD). For this study, a 50 mg of sample was used. The sample was pretreated in flowing 20 ml/min N_2 atmosphere at 250°C for 30 min prior to running the TPR experiment, and then cooled down to room temperature in N_2. A 5% H_2 in N_2 gas at a flow rate of 75 ml/min was used as a reducing gas. The sample temperature was raised at a constant rate of 10°C/min from room temperature to 950°C. The amount of H_2 consumption during the increasing temperature period was determined by using a TCD signal.

Temperature programmed oxidation was carried out in TPO micro-reactor coupled to a FID analyszer. The TPO was used to determine the amount of carbonaceous deposition on the used catalysts. After running the reaction at 750°C for 24 hr, the catalyst was cooled down to room temperature in He. Then, about 30 mg sample was heated in a $2\%O_2$ in He (40 ml/min) at a heating rate 10°C/min up to 900°C. The output gas was passed to a methanation reactor using 15 wt% Ni/Al_2O_3 as a catalyst prior to FID detector. After the system reached 900°C, 100 µl of CO_2 pulses were injected in order to calibrate the amount of coke on the catalyst.

7.3.3 Activity Tests

Catalytic activity tests for methane oxidation were carried out in a packed-bed quartz tube microreactor (i.d. 6 mm). Typically, a 100 mg of catalyst sample was packed between layers of quartz wool. The reactor was placed in an electric furnace equipped with K-type thermocouples. The catalyst bed temperature was monitored and controlled by Shinko temperature controllers. Feed gas mixtures containing $4\%CH_4$, $2\%O_2$ and balance He were used. The total flow rate of feed gas into the reactor was kept at 100 ml/min using Brooks mass flow controllers. The reactions were carried out at GHSV 50,000 hr^{-1}. The product gases were chromatographically analyzed using a Shimadzu GC 8A fitted with a thermal conductivity detector. A CTR I (Alltech) packed column was used to separate all products at 50°C except H_2O which was evaluated from the oxygen mole balance. Carbon balances were confirmed with all experiments conducted. The conversion of CH_4 (X_{CH_4}), O_2 consumption (X_{O_2}) and selectivities (S) reported in this work were calculated from:

$$\%X_{CH_4} = \frac{CH_4^{in} - CH_4^{out}}{CH_4^{in}} \times 100 \qquad (3.3)$$

$$\%X_{O_2} = \frac{O_2^{in} - O_2^{out}}{O_2^{in}} \times 100 \qquad (3.4)$$

$$\%S_{CO} = \frac{CO^{out}}{CO^{out} + CO_2^{out}} \times 100 \quad (3.5)$$

$$\%S_{H_2} = \frac{H_2^{out}}{H_2^{out} + H_2O^{out}} \times 100 \quad (3.6)$$

7.4 Results and Discussion

7.4.1 Catalyst Characterizations

7.4.1.1 BET Surface Area, Metal Dispersion

BET surface areas of the $Ce_{0.75}Zr_{0.25}O_2$, Nb-doped $Ce_{0.75}Zr_{0.25}O_2$ and Nb_2O_5 catalysts calcined at 500 and 900°C samples are summarized in Table 1. It was found that the surface area decreased with an increase in Nb loading. For samples calcined at 900°C, surface areas of Nb-doped mixed oxide samples are higher than that of $Ce_{0.75}Zr_{0.25}O_2$ which in turn suggested that the presence of Nb stabilizes the surface area of $Ce_{0.75}Zr_{0.25}O_2$. It should be noted that no hydrogen chemisorption was observed in the $Ce_{0.75}Zr_{0.25}O_2$, Nb-doped $Ce_{0.75}Zr_{0.25}O_2$ and Nb_2O_5 samples.

Table 7.1 BET surface areas of Nb-doped $Ce_{0.75}Zr_{0.25}O_2$ catalysts calcined at 500 and 900 °C

Catalysts	calcined at 500°C (m^2/g)	calcined at 900°C (m^2/g)
$Ce_{0.75}Zr_{0.25}O_2$	108.4	9.2
1%Nb-doped $Ce_{0.75}Zr_{0.25}O_2$	102.8	26.3
5%Nb-doped $Ce_{0.75}Zr_{0.25}O_2$	101.4	18.7
10%Nb-doped $Ce_{0.75}Zr_{0.25}O_2$	82.6	12.5
Nb_2O_5	62.5	13.1

The BET surface areas and Ni metal dispersion data of 5 wt% Ni over Nb-doped catalysts are shown in Table 7.2. It can be seen that the BET surface area and metal dispersion were decreased with an increasing amount of Nb loading. This result indicated that the exposed Ni atom to H_2 is depressed by Nb.

Table 7.2 BET surface area and degree of dispersion of 5 wt% Ni over Nb-doped $Ce_{0.75}Zr_{0.25}O_2$ catalysts calcined at 500°C

Catalyst	BET Surface Area (m^2/g)	Dispersion (%)
5%Ni/$Ce_{0.75}Zr_{0.25}O_2$	66	6.40
5%Ni/1%Nb-doped $Ce_{0.75}Zr_{0.25}O_2$	63	2.35
5%Ni/5%Nb-doped $Ce_{0.75}Zr_{0.25}O_2$	57	1.05
5%Ni/10%Nb-doped $Ce_{0.75}Zr_{0.25}O_2$	60	0.58

7.4.1.2 XRD

XRD patterns of Nb-doped $Ce_{0.75}Zr_{0.25}O_2$ mixed oxide catalysts after calcined at 500°C are shown in Figure 7.1. The data confirmed cubic phases of fluorite structure as the major crystalline phase and no crytallites of Fergusonite ($CeNbO_4$). The samples calcined at 900°C gave similar results, but with sharper peaks indicating larger particle sizes consistent with the lower specific surface areas.

The XRD patterns of 5 wt% Ni over Nb-doped $Ce_{0.75}Zr_{0.25}O_2$ catalysts are shown in Figure 7.2. The XRD patterns are similar to that of $Ce_{0.75}Zr_{0.25}O_2$ but the small peak of NiO was observed at ca. 47° (2θ). It should be note that no formation of Ni-Nb alloy or Ce-Nb alloys was observed.

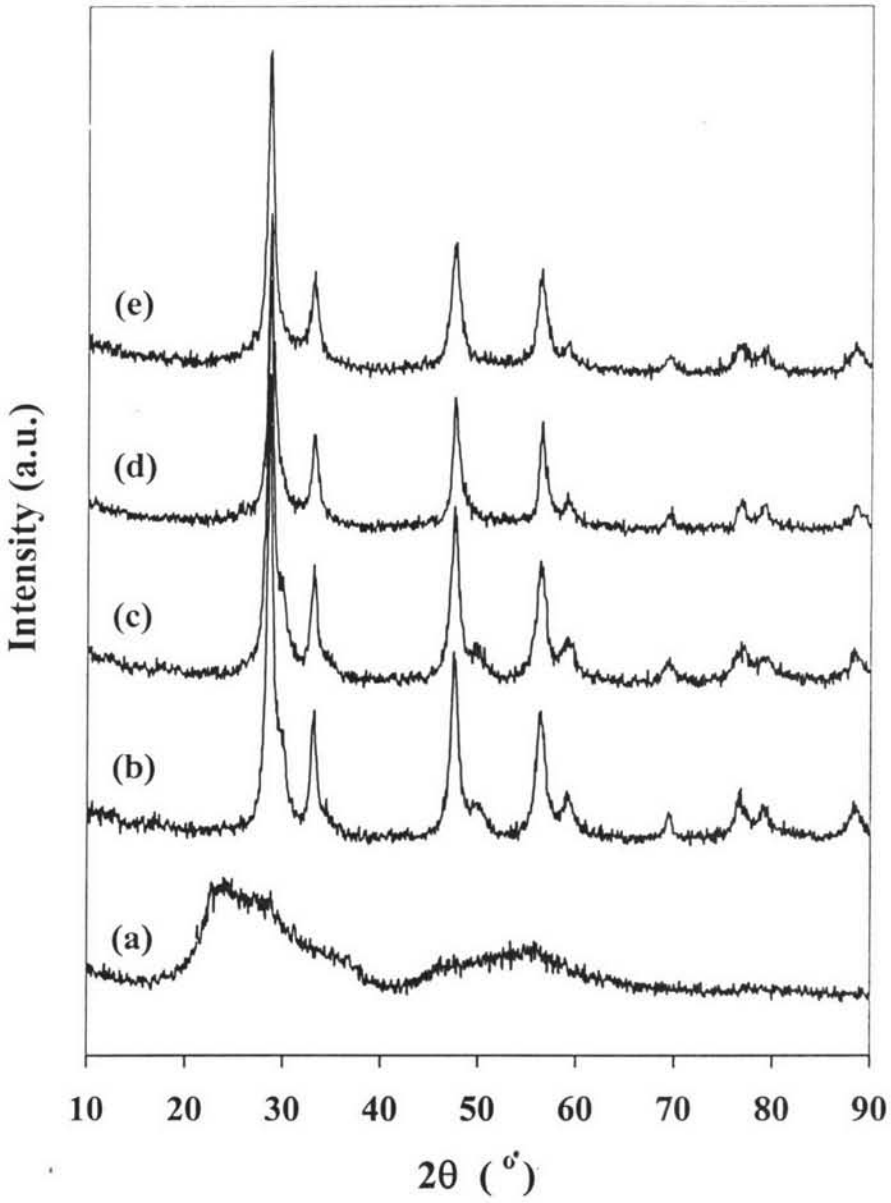

Figure 7.1 XRD patterns for Nb doped catalysts with the aging time of 50 h, and calcined at 500°C: (a) Nb_2O_5 (b) $Ce_{0.75}Zr_{0.25}O_2$ (c) 1%Nb-doped $Ce_{0.75}Zr_{0.25}O_2$ (d) 5%Nb-doped $Ce_{0.75}Zr_{0.25}O_2$ and (e) 10%Nb-doped $Ce_{0.75}Zr_{0.25}O_2$.

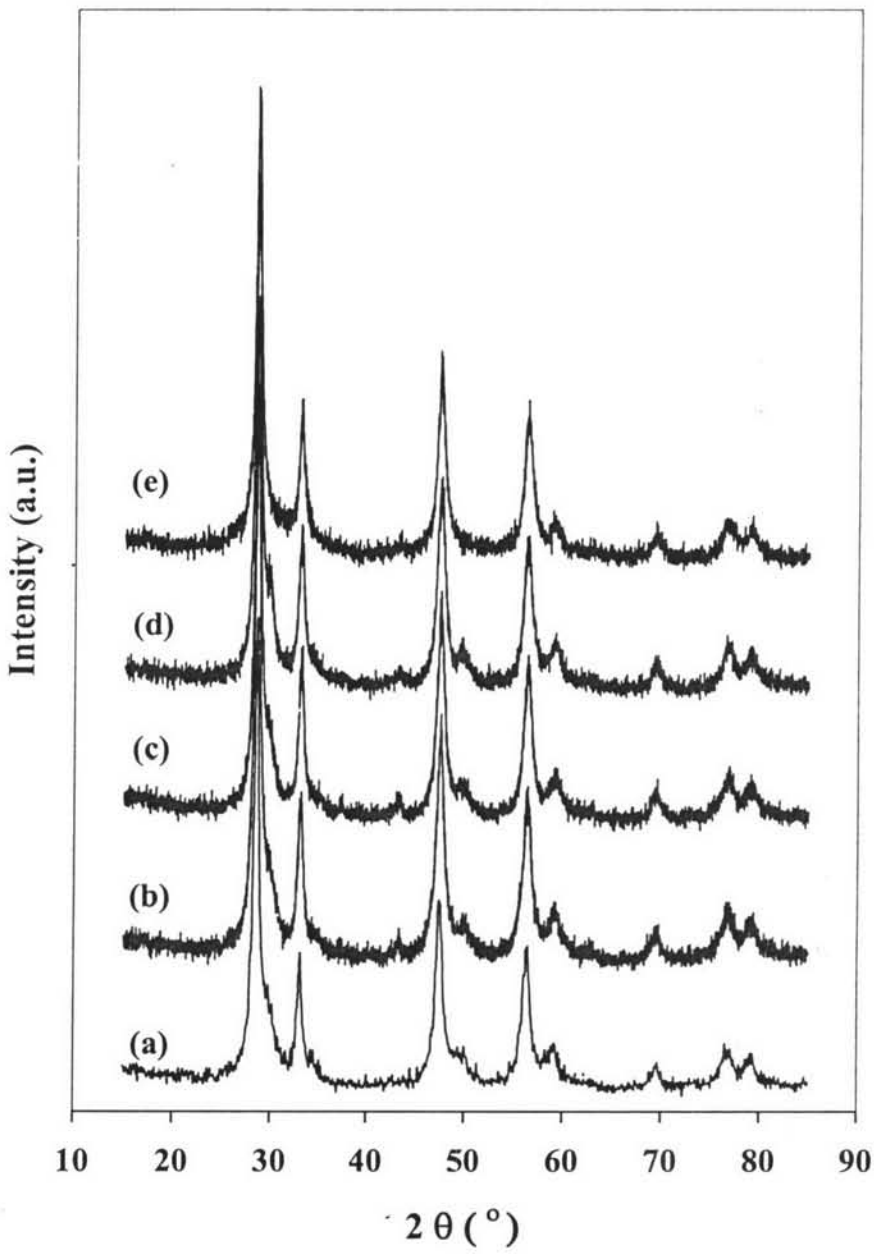

Figure 7.2 XRD patterns for Ni over Nb doped catalysts with the aging time of 50 h, and calcined at 500°C: (a) $Ce_{0.75}Zr_{0.25}O_2$ (b) 5 wt% Ni/$Ce_{0.75}Zr_{0.25}O_2$ (c) 5 wt% Ni/1%Nb-doped $Ce_{0.75}Zr_{0.25}O_2$ (d) 5 wt% Ni/5%Nb-doped $Ce_{0.75}Zr_{0.25}O_2$ and (e) 5 wt% Ni/10%Nb-doped $Ce_{0.75}Zr_{0.25}O_2$.

7.4.1.3 H_2 - TPR

Reducibility of the samples was investigated using H_2-TPR technique. Figure 7.3 shows the H_2-TPR profiles of $Ce_{0.75}Zr_{0.25}O_2$, Nb-doped $Ce_{0.75}Zr_{0.25}O_2$ and Nb_2O_5 calcined at 500°C. For $Ce_{0.75}Zr_{0.25}O_2$, two peaks are observed at lower and higher temperature regions. The first peak in the low temperature region is the reduction of surface oxygen and the other peak is the reduction of bulk oxygen (Luo and Zheng, 1999; Otsuka *et al.*, 1999). For the H_2-TPR profile of Nb_2O_5, it can be seen that the reduction of the sample occurred at temperature higher than 800°C since Nb_2O_5 is difficult to reduce (Wachs *et al.*, 2000). As can be seen in Figure 7.3, the introduction of Nb modifies the reduction behaviour of $Ce_{0.75}Zr_{0.25}O_2$ mixed oxides. The H_2-TPR profile for 1 wt% Nb-doped $Ce_{0.75}Zr_{0.25}O_2$ mixed oxide is similar to that of $Ce_{0.75}Zr_{0.25}O_2$ but the reduction temperature of the 1 wt% Nb-doped $Ce_{0.75}Zr_{0.25}O_2$ mixed oxide was shifted to lower temperatures (450°C). On the other hand, each of the first peak for the H_2-TPR profiles of 5 and 10 wt% Nb-doped samples is shifted to higher temperature compared with that of the 1 wt% Nb-doped sample. These indicated that 1 wt% Nb loading can improve the reducibility of $Ce_{0.75}Zr_{0.25}O_2$ mixed oxide while increasing the amount of Nb (5 and 10 wt%) slightly retarded the surface oxygen reducibility of $Ce_{0.75}Zr_{0.25}O_2$ mixed oxide.

The H_2-TPR profiles of the samples calcined at 900°C (Figure 7.4) are still similar to those of samples calcined at 500°C but were shifted to higher temperatures. Moreover, the amounts of H_2 uptake over the samples calcined at 900°C are smaller than that of samples calcined at 500°C except for 1 wt% Nb-doped $Ce_{0.75}Zr_{0.25}O_2$ sample. It is apparent that the introduction of 1 wt% of Nb into $Ce_{0.75}Zr_{0.25}O_2$ stabilizes its redox properties.

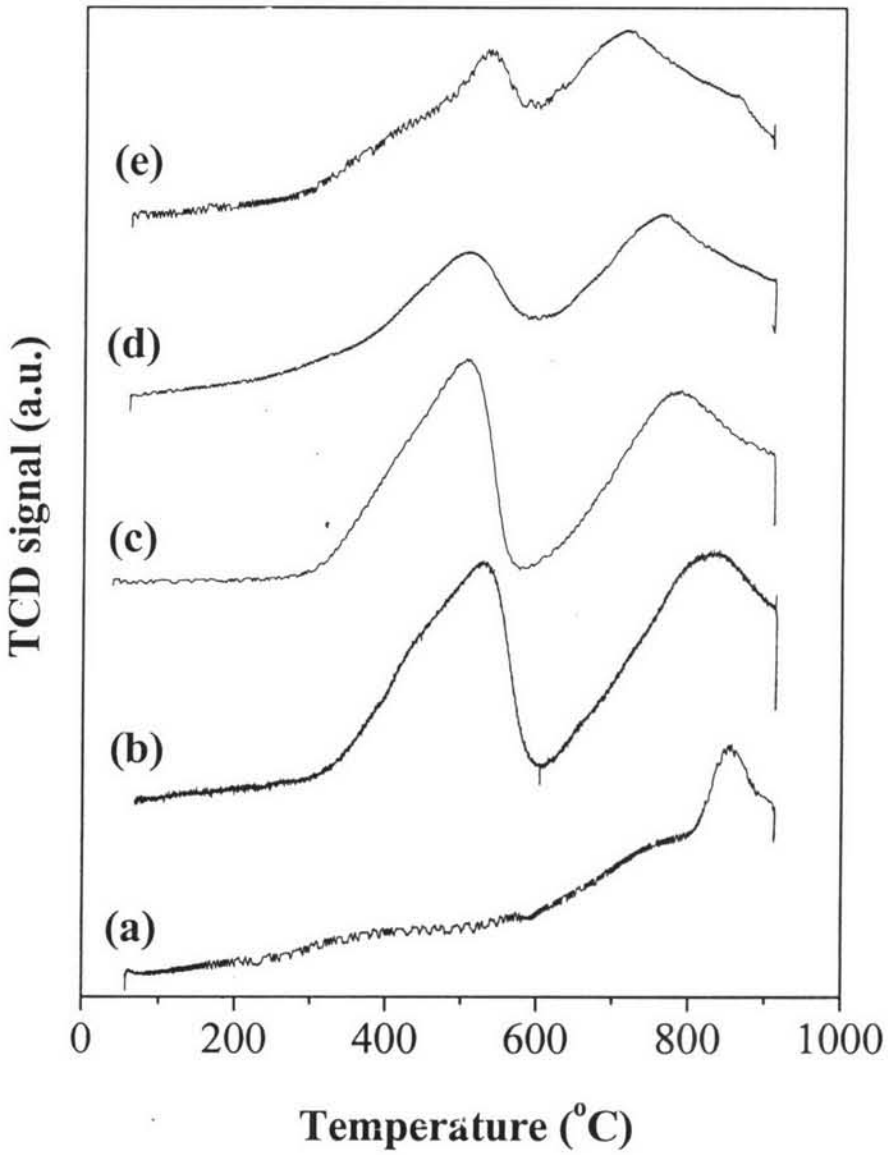

Figure 7.3 TPR profiles of Nb-doped catalysts calcined at 500°C, a reducing gas containing 5% H_2 in helium and a heating rate of 10°C min^{-1}, with a gas flow rate of 50 *ml* min^{-1}: (a) Nb_2O_5 (b) $Ce_{0.75}Zr_{0.25}O_2$ (c) 1%Nb-doped $Ce_{0.75}Zr_{0.25}O_2$ (d) 5%Nb-doped $Ce_{0.75}Zr_{0.25}O_2$ (e) 10%Nb-doped $Ce_{0.75}Zr_{0.25}O_2$.

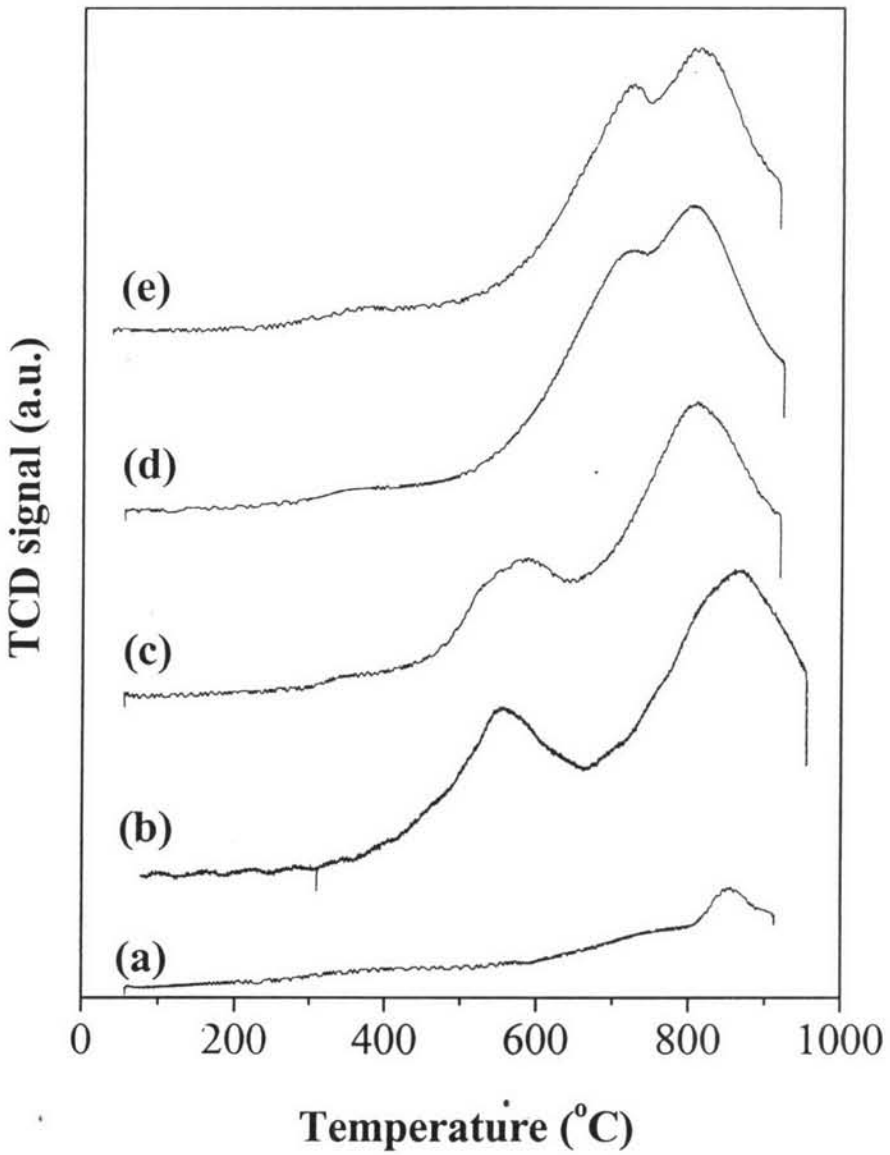

Figure 7.4 TPR profiles of Nb-doped catalysts calcined at 900°C, a reducing gas containing 5% H_2 in helium and a heating rate of 10°C min^{-1}, with a gas flow rate of 50 *ml* min^{-1}: (a) Nb_2O_5 (b) $Ce_{0.75}Zr_{0.25}O_2$ (c) 1%Nb-doped $Ce_{0.75}Zr_{0.25}O_2$ (d) 5%Nb-doped $Ce_{0.75}Zr_{0.25}O_2$ (e) 10%Nb-doped $Ce_{0.75}Zr_{0.25}O_2$.

Figure 7.5 shows the H_2-TPR profiles of Ni over Nb-doped $Ce_{0.75}Zr_{0.25}O_2$ catalysts calcined at 500°C prepared by impregnation. For the profile of 5 wt% $Ni/Ce_{0.75}Zr_{0.25}O_2$, it can be seen that the reduction peaks of the sample occurred at temperature ≈ 300, 370°C and other broad peak at temperature over 800°C. The first two peaks indicate the reduction of NiO to Ni^0 and the other is the reduction of support (Montoya *et al.*, 2000). The peak at lower temperature (ca. 300°C) seems to disappear while the other peak (ca. 370°C) becomes more broad and weaker with increasing in amount of Nb. Generally, for supported Ni catalysts the lower temperature peaks are attributed to the reduction of the relatively free NiO particles, while the higher temperature peaks are the reduction of complex NiO species in intimate contact with the oxide support (Roh *et al.*, 2002). This indicates that the Nb species may be mainly associated with NiO resulting to retard the NiO reduction. Furthermore, an addition peak was found at temperature about 500°C and became to significantly increase while the NiO reduction peak at temperature about 370°C was decreased with an increase of Nb loadings. By comparing with their supports (Figure 7.3), the addition peak at temperature about 500°C is the surface oxygen reduction and was shifted to lower temperature by loaded Ni. This may be caused by the hydrogen spillover effect enhanced by metallic Ni particles formed by the NiO reduction (Takeguchi *et al.*, 2001). This behavior is generally observed in the presence of Ni and platinum-group metal.

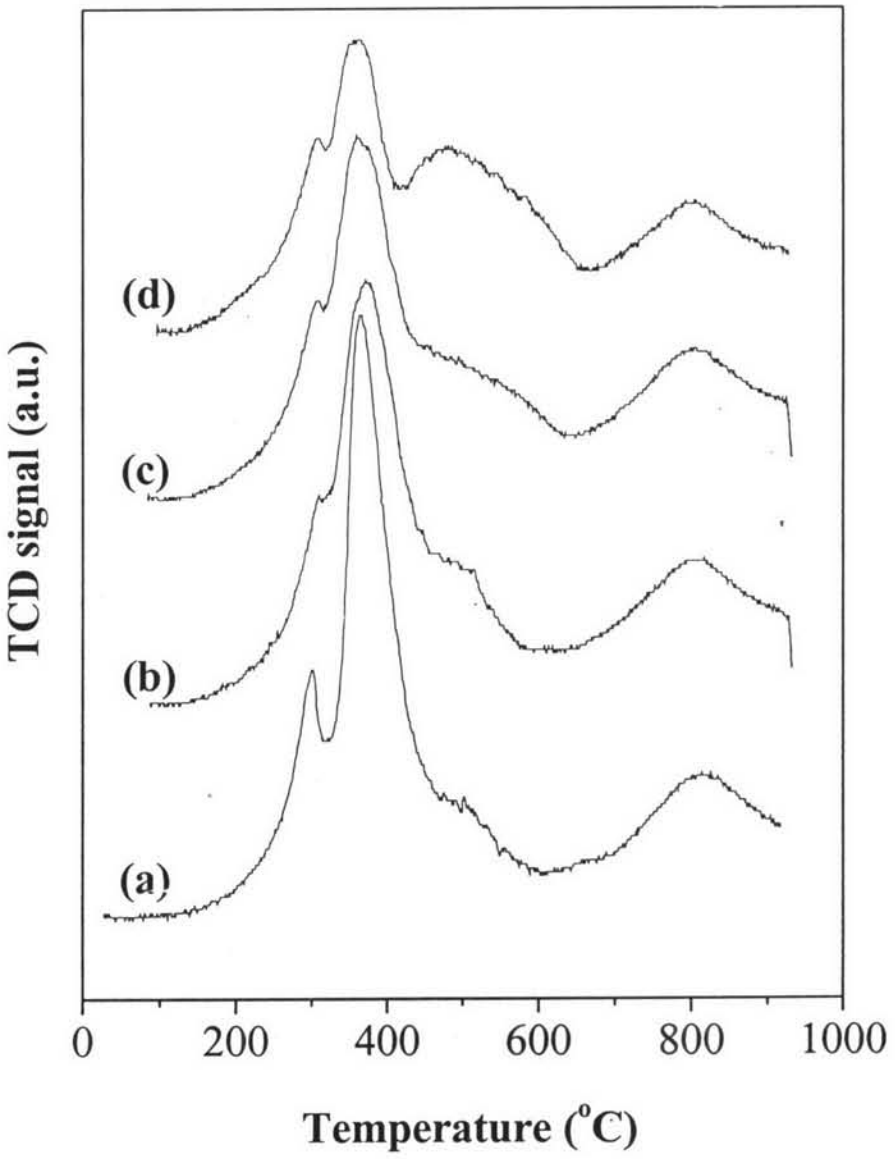

Figure 7.5 TPR profiles of Ni over Nb-doped $Ce_{0.75}Zr_{0.25}O_2$ catalysts calcined at 500°C, a reducing gas containing 5% H_2 in helium and a heating rate of 10°C min^{-1}, with a gas flow rate of 50 *ml* min^{-1}: (a) 5 wt% Ni/$Ce_{0.75}Zr_{0.25}O_2$ (c) 5 wt% Ni/1%Nb-doped $Ce_{0.75}Zr_{0.25}O_2$ (d) 5 wt% Ni/5%Nb-doped $Ce_{0.75}Zr_{0.25}O_2$ (e) 5 wt% Ni/10%Nb-doped $Ce_{0.75}Zr_{0.25}O_2$.

7.4.2 Catalytic Activity Test

Figures 7.6 and 7.7 show the methane conversion and product selectivities as functions of temperature for methane partial oxidation over Ni/Nb-doped $Ce_{0.75}Zr_{0.25}O_2$ catalysts calcined at 500°C.

For the 5 wt% $Ni/Ce_{0.75}Zr_{0.25}O_2$ catalyst, synthesis gas started to form at temperatures above 550°C. Adding Nb caused the light-off temperature to shift to higher temperatures. For low amount of Nb loadings (1 wt%), synthesis gas was started at temperature above 600°C and shifted to higher temperatures with increasing amount of Nb loadings. This might be due to lower reducibility and metal dispersion on the Ni/Nb-doped $Ce_{0.75}Zr_{0.25}O_2$ catalysts. The decrease of catalyst activity with increasing the amount of Nb loading could be associated with the apparent increase in Ce^{3+}, where its degree of reducibility is low. This finding is in agreement with Nb-doped ceria reported by Ramirez-Cabrera *et al.* (2002).

7.4.3 Carbon Deposition

The amount of carbon deposition on the catalysts after 24 h of reaction at 750°C and CH_4/O_2 ratio of 2 are shown in Table 7.3. The amount of carbon deposition on the spent catalysts was quantified by TPO technique. As shown in Table 7.3, the amount of carbon deposition was found to increase sharply by more than 50% with small amounts of Nb loadings. This indicated that the carbon deposition is strongly produced in the presence of Nb. It seem to be that the amount of carbon deposition on the catalyst was more pronounced by increasing amount of Nb loading.

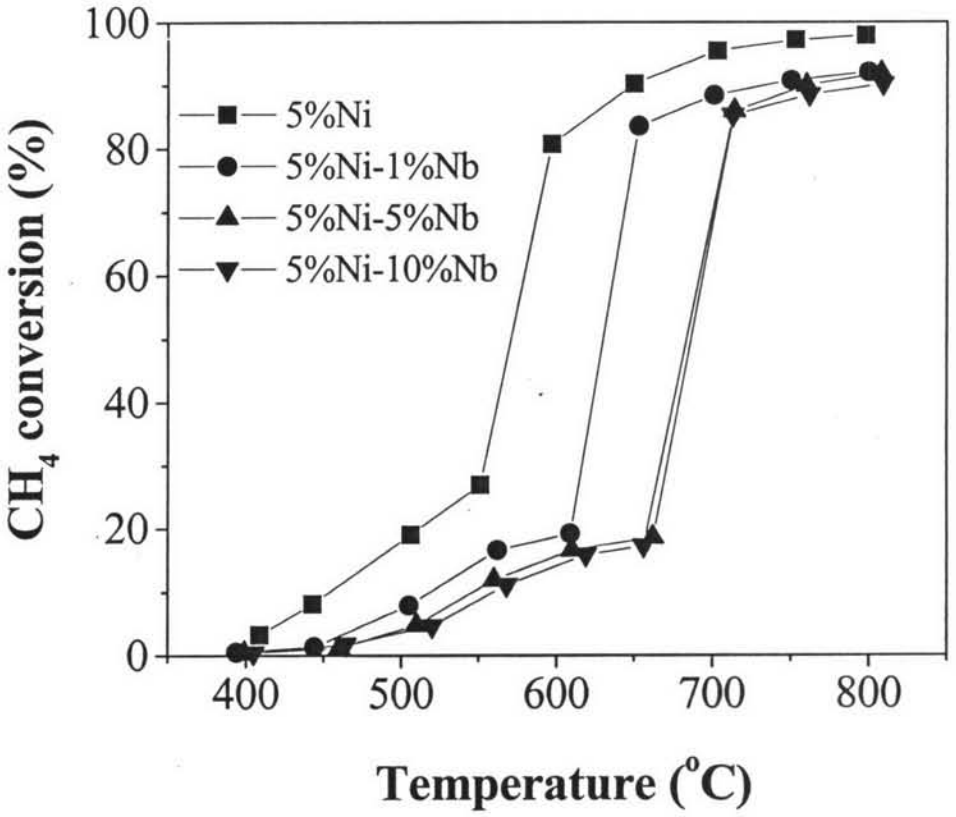

Figure 7.6 Methane conversion at different temperature for methane partial oxidation over Ni/Nb-doped $Ce_{0.75}Zr_{0.25}O_2$ catalysts (CH_4/O_2 ratio of 2.0, GHSV = 53,000 h^{-1}).

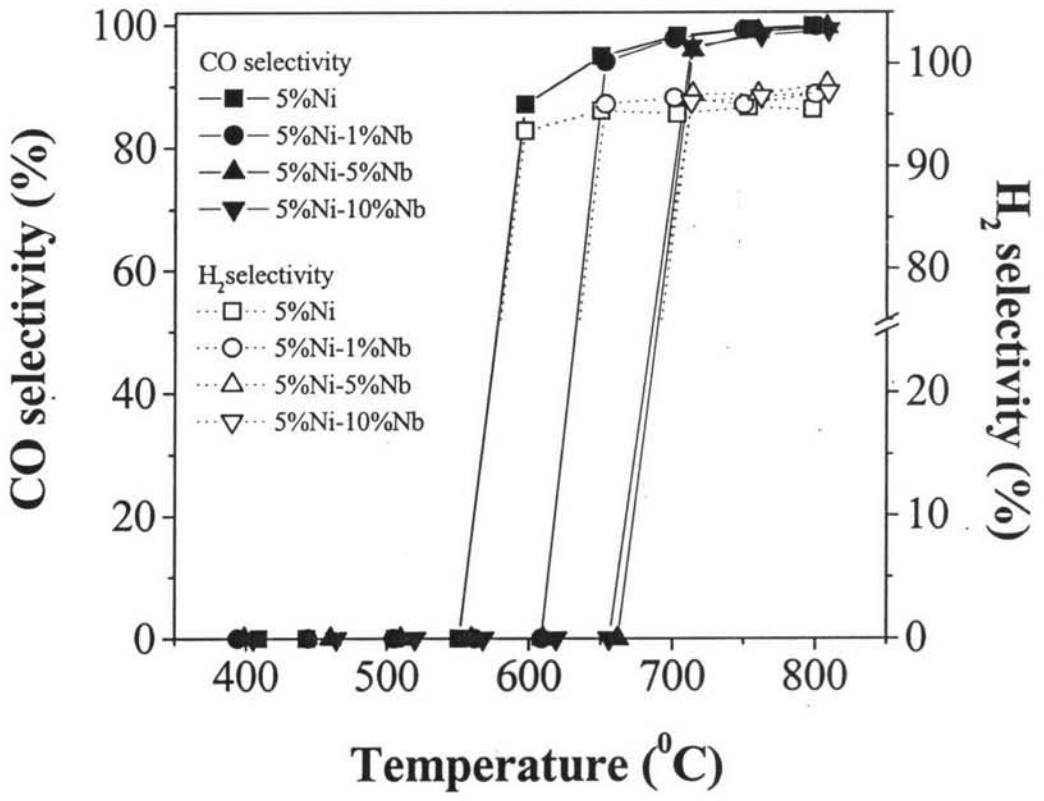

Figure 7.7 CO and H_2 selectivities at different temperature for methane partial oxidation over Ni/Nb-doped $Ce_{0.75}Zr_{0.25}O_2$ catalysts (CH_4/O_2 ratio of 2.0, GHSV = 53,000 h^{-1}).

Table 7.3 The amount of carbon deposition quantified by TPO over the Ni/Nb-doped $Ce_{0.75}Zr_{0.25}O_2$ catalysts after 24 hr of reaction at 750^0C and CH_4/O_2 ratio of 2.0

Catalyst	CH_4 Conversion[1] (%)	Amount of carbon deposition (wt%)
5% $Ni/Ce_{0.75}Zr_{0.25}O_2$	97	8.19
5%Ni/1%Nb-doped	90	22.8
5%Ni/5%Nb-doped	87	27.6
5%Ni/10%Nb-doped	85	37.7

[1]at the end of reaction time (24hr)

7.5 Conclusions

It can be concluded that the catalytic activity for methane partial oxidation of the catalysts studied depends on the incorporation of Nb loading. The Nb loadings virtually inhibit the catalytic activity of $Ni/Ce_{0.75}Zr_{0.25}O_2$ catalyst. It was found that the catalytic activities for methane and iso-octane partial oxidation were decreased with an increasing amount of Nb loadings. Moreover, the amount of carbon deposition was increased with an increase of Nb loadings. This might be due to inhibition of the surface oxygen reduction of $Ce_{0.75}Zr_{0.25}O_2$, reduction of interaction with support and high acidity of NbO_x.

7.6 Acknowledgements

The authors would like to thank Royal Golden Jubilee Ph.D. program, Thailand Research Fund and Ratchadapiseksomphote Fund, CU for the financial support.

7.7 References

Barbieri, F., Cauzzi, D., Smet, F.D., Devillers, M., Moggi, P., Predieri, G., Ruiz; P. (2000) Mixed Oxide Catalysts Involving V, Nb and Si Obtained by a Non-Hydrolytic Sol-gel Route: Preparation and Catalytic Behaviour in Oxydative Dehydrogenation of Propane. Catalysis Today, 61, 353.

Jehng, J. M., Wachs, I.E. (1993) Molecular Design of Supported Niobium Oxide Catalysts. Catalysis Today, 16, 417.

Luo, M. Zheng, X. (1999) Redox Behaviour and Catalytic Properties of $Ce_{0.5}Zr_{0.5}O_2$-Supported Palladium Catalysts. Applied Catalysis A: General, 189, 15.

Montoya, J.A., Romero-Pascual, E., Gimon, C., Del Angle, P., Monzon, A., (2000) Methane Reforming with CO_2 over Ni/ZrO_2-CeO_2 Catalysts Prepared by Sol-Gel. Catalysis Today, 63, 71.

Noronha F. B., Aranda, D.A.G., Ordine A.P., Schmal, M. (2000) The Promoting Effect of Nb_2O_5 Addition to Pd/Al_2O_3 Catalysts on Propane Oxidation. Catalysis Today, 57, 275.

Otsuka K., Wang Y. and Nakamura M., (1999) Direct conversion of methane to synthesis gas through gas-solid reaction using CeO_2-ZrO_2 solid solution at moderate temperature. Applied Catalysis A: General, 183, 317.

Pengpanich S., Meeyoo V., Rirksomboon T. and Bunyakiat K. (2002) Catalytic oxidation of methane over CeO_2-ZrO_2 mixed oxide solid solution catalysts prepared via urea hydrolysis. Applied Catalysis A: General, 234, 221.

Ramirez-Cabrera, E., Atkinson, A., Chadwick, D., (2002) Reactivity of Ceria, Gd- and Nb-Doped Ceria to Methane. Applied Catalysis B: Environmental, 36, 193.

Roh. H., Jun, K., Dong, W., Chang, J., Park, S., and Joe, Y. (2002) Highly Active and Stable Ni/Ce-ZrO_2 Catalyst for H_2 Production from Methane. Journal of Molecular Catalysis A: Chemical, 181, 137

Stagg-Williams, S.M., Noranha, F.B., Fendley, G., Resasco, D.E. (2000) CO_2 Reforming of CH_4 over Pt/ZrO_2 Catalysts Promoted with La and Ce Oxides. Journal of Catalysis, 194, 240.

Takeguchi, T., Furukawa, S., and Inoue, M. (2001) Hydrogen Spillover from NiO to the Large Surface Area CeO_2-ZrO_2 Solid Solutions and Activity of the NiO/CeO_2-ZrO_2 Catalysts for Partial Oxidation of Methane. Journal of Catalysis, 202,14.

Wachs I. E., Jehng, J.M., Deo, G., Hu, H., Arora, N. (1996) Redox Properties of Niobium Oxide Catalysts. Catalysis Today, 28, 199.